Research Article | Vol. 26, No. 2 | 22 Jan 2018 | OPTICS EXPRESS 687
Optics EXPRESS

Dynamic phase extraction in a modulated double-pulse ϕ-OTDR sensor using a stable homodyne demodulation in direct detection

YONAS MUANENDA,* STEFANO FARALLI, CLAUDIO J. OTON, AND FABRIZIO DI PASQUALE

Institute of Information Communication and Perception Technologies, Scuola Superiore Sant' Anna, Via G. Moruzzi 1, 56124 Pisa, Italy
**y.muanenda@sssup.it*

Abstract: We propose and experimentally demonstrate a stable homodyne phase demodulation technique in a ϕ-OTDR using a double-pulse probe and a simple direct detection receiver. The technique uses selective phase modulation of one of a pair of pulses to generate a carrier for dynamic phase changes and involves an enhanced phase demodulation scheme suitable for distributed sensing by being robust against light intensity fluctuations, independent of the modulation depth, and convenient for analogue signal processing. The capability of the technique to quantify distributed dynamic phase change due to a generic external impact is experimentally demonstrated by measuring the phase change induced by a nonlinear actuator generating a 2 kHz perturbation at a distance of 1.5 km on a standard singlemode fiber with an SNR of ~24 dB. The demodulated nonlinear response is shown to have a spectrum consistent with one obtained using an FBG sensor and a commercial reading unit.

OCIS codes: (060.2370) Fiber optics sensors; (060.4370) Nonlinear optics, fibers; (290.5870) Scattering, Rayleigh; (120.4825) Optical time domain reflectometry; (120.5050) Phase measurement.

References and links

1. K. Johannessen and B. K. Drakeley, "Distributed Acoustic Sensing: a new way of listening to your well/reservoir," SPE Intelligent Energy International, SPE-149602-MS (2012).
2. Persistence Market Research forecast, "Global Distributed Acoustic Sensing Market to Surpass US$ 2 Billion in Revenues by 2025," (Persistence Market Research, 2017) http://www.persistencemarketresearch.com/mediarelease/distributed-acoustic-sensing-market.asp.
3. J. Park and H. F. Taylor, "Fiber Optic Intrusion Sensor using Coherent Optical Time Domain Reflectometer," Jpn. J. Appl. Phys. **42**(1), 3481–3482 (2003).
4. J. C. Juarez, E. W. Maier, K. N. Choi, and H. F. Taylor, "Distributed fiberoptic intrusion sensor system," J. Lightwave Technol. **23**(6), 2081–2087 (2005).
5. Z. Qin, L. Chen, and X. Bao, "Continuous wavelet transform for non-stationary vibration detection with phase-OTDR," Opt. Express **20**(18), 20459–20465 (2012).
6. Y. Muanenda, C. J. Oton, S. Faralli, and F. Di Pasquale, "A Cost-Effective Distributed Acoustic Sensor Using a Commercial Off-the-Shelf DFB Laser and Direct Detection Phase-OTDR," IEEE Photonics J. **8**(1), 1–10 (2016).
7. Y. Muanenda, C. J. Oton, S. Faralli, T. Nannipieri, A. Signorini, and F. Di Pasquale, "Hybrid distributed acoustic and temperature sensor using a commercial off-the-shelf DFB laser and direct detection," Opt. Lett. **41**(3), 587–590 (2016).
8. Z. Qin, T. Zhu, L. Chen, and X. Bao, "High Sensitivity Distributed Vibration Sensor Based on Polarization-Maintaining Configurations of Phase-OTDR," IEEE Photonics Technol. Lett. **23**(15), 1091–1093 (2011).
9. Y. Koyamada, M. Imahama, K. Kubota, and K. Hogari, "Fiber-optic distributed strain and temperature sensing with very high measurand resolution over long range using coherent OTDR," J. Lightwave Technol. **27**(9), 1142–1146 (2009).
10. A. Garcia-Ruiz, J. Pastor-Graells, H. F. Martins, S. Martin-Lopez, and M. Gonzalez-Herraez, "Speckle analysis method for distributed detection of temperature gradients with phi-OTDR," IEEE Photonics Technol. Lett. **28**(18), 2000–2003 (2016).
11. J. Pastor-Graells, H. F. Martins, A. Garcia-Ruiz, S. Martin-Lopez, and M. Gonzalez-Herraez, "Single-shot distributed temperature and strain tracking using direct detection phase-sensitive OTDR with chirped pulses," Opt. Express **24**(12), 13121–13133 (2016).

#306028 https://doi.org/10.1364/OE.26.000687
Journal © 2018 Received 8 Sep 2017; revised 17 Nov 2017; accepted 24 Nov 2017; published 9 Jan 2018

Optics EXPRESS

12. A. Garcia-Ruiz, J. Pastor-Graells, H. F. Martins, K. Hey Tow, L. Thévenaz, S. Martin-Lopez, and M. Gonzalez-Herraez, "Distributed photothermal spectroscopy in microstructured optical fibers: towards high-resolution mapping of gas presence over long distances," Opt. Express **25**(3), 1789–1805 (2017).
13. S. Liehr, Y. S. Muanenda, S. Münzenberger, and K. Krebber, "Relative change measurement of physical quantities using dual-wavelength coherent OTDR," Opt. Express **25**(2), 720–729 (2017).
14. A. Masoudi, M. Belal, and T. P. Newson, "A distributed optical fibre dynamic strain sensor based on phase OTDR," Meas. Sci. Technol. **24**(8), 085204 (2013).
15. A. Masoudi and T. P. Newson, "High spatial resolution distributed optical fiber dynamic strain sensor with enhanced frequency and strain resolution," Opt. Lett. **42**(2), 290–293 (2017).
16. A. E. Alekseev, V. S. Vdovenko, B. G. Gorshkov, V. T. Potapov, and D. E. Simikin, "A phase-sensitive optical time-domain reflectometer with dual-pulse phase modulated probe signal," Laser Phys. **24**(11), 115106 (2014).
17. J. He, L. Wang, F. Li, and Y. Liu, "An Ameliorated Phase Generated Carrier Demodulation Algorithm With Low Harmonic Distortion and High Stability," J. Lightwave Technol. **28**(22), 3258–3265 (2010).
18. S. C. Huang and H. Lin, "Modified phase-generated carrier demodulation compensated for the propagation delay of the fiber," Appl. Opt. **46**(31), 7594–7603 (2007).
19. F. Wang, J. Xie, Z. Hu, S. Xiong, H. Luo, and Y. Hu, "Interrogation of Extrinsic Fabry–Perot Sensors Using Path-Matched Differential Interferometry and Phase Generated Carrier Technique," J. Lightwave Technol. **33**(12), 2392–2397 (2015).
20. Y. Li, Z. Liu, Y. Liu, L. Ma, Z. Tan, and S. Jian, "Interferometric vibration sensor using phase-generated carrier method," Appl. Opt. **52**(25), 6359–6363 (2013).
21. X. Fang, "Fiber-optic distributed sensing by a two-loop Sagnac interferometer," Opt. Lett. **21**(6), 444–446 (1996).
22. Y. Liu, J. Jia, P. Tao, G. Yin, Z. Tan, W. Ren, and S. Jian, "Signal processing of Sagnac fiber interferometer used as distributed sensor with wavelets," in *Proceedings of Asia Communications and Photonics Conference and Exhibition* (IEEE, 2010), pp. 290–291.
23. A. Dandridge, A. B. Tveten, and T. G. Giallorenzi, "Homodyne Demodulation Scheme for Fiber Optic Sensors Using Phase Generated Carrier," IEEE Trans. Microw. Theory Tech. **30**(10), 1635–1641 (1982).
24. C. McGarrity and D. A. Jackson, "Improvement on phase generated carrier technique for passive demodulation of miniature interferometric sensors," Opt. Commun. **109**(3–4), 246–248 (1994).
25. Y. Liu, L. W. Wang, C. D. Tian, M. Zhang, and Y. B. Liao, "Analysis and optimization of the PGC method in all digital demodulation systems," J. Lightwave Technol. **26**(18), 3225–3233 (2008).
26. J. He, L. Wang, F. Li, and Y. Liu, "An Ameliorated Phase Generated Carrier Demodulation Algorithm With Low Harmonic Distortion and High Stability," J. Lightwave Technol. **28**(22), 258–3265 (2010).
27. A. Zhang and S. Zhang, "High Stability Fiber-Optics Sensors With an Improved PGC Demodulation Algorithm," IEEE Sens. J. **16**(21), 7681–7684 (2016).
28. Q. Kemao, W. Gao, and H. Wang, "Windowed Fourier-filtered and quality-guided phase-unwrapping algorithm," Appl. Opt. **47**(29), 5420–5428 (2008).
29. J. A. Langley, R. G. Brice, and Q. Zhao, "Recursive approach to the moment-based phase unwrapping method," Appl. Opt. **49**(16), 3096–3101 (2010).
30. J. Weng and Y. Lo, "Novel rotation algorithm for phase unwrapping applications," Opt. Express **20**(16), 16838–16860 (2012).
31. Z. Cheng, D. Liu, Y. Yang, T. Ling, X. Chen, L. Zhang, J. Bai, Y. Shen, L. Miao, and W. Huang, "Practical phase unwrapping of interferometric fringes based on unscented Kalman filter technique," Opt. Express **23**(25), 32337–32349 (2015).
32. G. Dardikman, S. Mirsky, M. Habaza, Y. Roichman, and N. T. Shaked, "Angular phase unwrapping of optically thick objects with a thin dimension," Opt. Express **25**(4), 3347–3357 (2017).
33. D. Kitahara, M. Yamagishi, and I. Yamada, "A virtual resampling technique for algebraic two-dimensional phase unwrapping," in *Proceedings of 2015 IEEE International Conference on Acoustics, Speech and Signal Processing* (IEEE, 2015), pp. 3871–3875.
34. N. H. Ching, D. Rosenfeld, and M. Braun, "Two-dimensional phase unwrapping using a minimum spanning tree algorithm," IEEE Trans. Image Process. **1**(3), 355–365 (1992).
35. H. Liu, M. Xing, and Z. Bao, "A Cluster-Analysis-Based Noise-Robust Phase-Unwrapping Algorithm for Multibaseline Interferograms," IEEE Trans. Geosci. Remote Sens. **53**(1), 494–504 (2015).
36. D. M. Scott, *Industrial Process Sensors* (CRC Press, 2008).
37. M. G. Guvench, M. Miske, and E. Crain, "Design, fabrication and testing of CMOS operational amplifiers as training tool in analog integrated circuit design," in *Proceedings of the Fourteenth Biennial University/ Government/ Industry Microelectronics Symposium* (IEEE, 2001), pp. 193–196.
38. A. C. B. Albason, N. M. L. Axalan, M. T. A. Gusad, J. R. E. Hizon, and M. D. Rosales, "Design Methodologies for Low-Power CMOS Operational Amplifiers in a 0.25μm Digital CMOS Process," in *Proceedings of TENCON 2006 - 2006 IEEE Region 10 Conference* (IEEE, 2006), pp. 1–4.
39. C. Kopp, C. Kopp, S. Bernabé, B. B. Bakir, J. Fedeli, R. Orobtchouk, F. Schrank, H. Porte, L. Zimmermann, and T. Tekin, "Silicon Photonic Circuits: On-CMOS Integration, Fiber Optical Coupling, and Packaging," IEEE J. Sel. Top. Quantum Electron. **17**(3), 498–509 (2011).
40. D. Okamoto, Y. Suzuki, K. Yashiki, Y. Hagihara, M. Tokushima, J. Fujikata, M. Kurihara, J. Tsuchida, T. Nedachi, J. Inasaka, and K. Kurata, "25-Gbps 5×5 mm chip-scale silicon-photonic receiver integrated with 28-

Optics EXPRESS

nm CMOS transimpedance amplifier," in *Proceedings of 2015 IEEE Optical Interconnects Conference* (IEEE, 2015), pp. 56–57.
41. L. S. Christensen and D. Manvell, "Sound level meters in building acoustic measurements," J. Build. Acoust. **5**(3), 217–222 (1998).
42. F. Bettarello, P. Fausti, V. Baccan, and M. Caniato, "Impact sound pressure level performances of basic beam floor structures," J. Build. Acoust. **17**(4), 305–316 (2010).
43. J. Torres and H. H. Asada, "Harmonic analysis of a PZT poly-actuator," in *Proceedings of IEEE International Conference on Robotics and Automation* (IEEE, 2015), pp. 842–849.
44. M. Ren, P. Lu, L. Chen, and X. Bao, "Study of Φ-OTDR stability for dynamic strain measurement in piezoelectric vibration," Photonic Sensors **6**(3), 199–208 (2016).

1. Introduction

Recently, fiber optic sensing for distributed dynamic monitoring has become a subject of detailed investigation, thanks mainly to the interesting applications it has in real-time monitoring of fast perturbations. Specifically, Distributed Acoustic Sensing (DAS), which involves the use of coherent Rayleigh backscattering in an optical fiber to determine multiple vibrations over an extended region, has become an effective and reliable technique owing to its capability to determine external acoustic impacts over long distances [1]. Recent survey shows that the global market share of DAS is steadily increasing and is projected to surpass $ 2bn in revenues by 2025 [2]. The technique has a number of interesting applications in many industrial fields including, among others, the monitoring of safety and integrity of large structures, oil & gas pipelines and railways infrastructures.

Phase-sensitive Optical Time Domain Reflectometry (ϕ-OTDR) is a sensing scheme commonly used for DAS and is based on the observation of phase-sensitive coherent Rayleigh speckles in time domain. In this scheme, pulses from a coherent light source which are sent into a sensing fiber result in coherent Rayleigh backscattering exhibiting a distributed speckle pattern sensitive to local phase changes induced by external impacts [3–8]. A local disturbance applied to the optical fiber causes a change in the refractive index and optical path length of the light passing through it, which in turn change the intensity and phase of the backscattering signal. Observing the evolution of the received signal for each spatial location reveals information on the distributed impact. The theoretical limit to the frequency of the impact signal that can be extracted is set by the round-trip time (RTT) of light along the fiber, making the technique suitable for high frequency vibration measurements. A number of techniques have been proposed to extract perturbations in ϕ-OTDR, most of them focusing on the measurement of the location, amplitude and frequency of the received signal, on which part of the information on the disturbance can be encoded. Early implementations include intrusion detection [3] using a simple direct detection scheme and extracting presence of impact with a differential intensity trace [4]. Other schemes involving the resolution of the backscattered signal in the wavelet domain have also been proposed [5]. More recent schemes use advanced signal processing to increase the signal-to-noise ratio of the backscattering signal in the measurement of vibration [6,7].

One of the issues in most existing ϕ-OTDR schemes is that measurement of the amplitudes of the backscattering signal alone does not provide all required quantitative information on the external impact. Quantitative measurement of any induced perturbation requires extracting the phase of the backscattering signal for each location as well. One of the first systems addressing this issue used coherent detection involving mixing of the backscattered signal at the receiver with a local oscillator and subsequent demodulation of the phase using a coherent receiver [8]. However, in such a scheme, polarization of the backscattered light is not controlled along the fiber and the resulting mixing with an optical local oscillator requires expensive polarization maintaining components. Recently, there have also been some investigations of phase demodulation in ϕ-OTDR using a direct detection receiver. One such scheme involves scanning the frequency of the pulses sent into the optical fiber and exploiting the duality of the change in the instantaneous frequency of the pulses and a change in refractive index caused by an external impact [9]. Correlations of a number of

Optics EXPRESS

traces at different frequency offsets from a reference trace taken at an unperturbed instant are made, and the frequency offset of the peak of the correlations is used to retrieve the local change in strain or temperature. However, this sensing technique is inherently quasi-static as it involves necessary waiting time for frequency scanning. Using a method which is based on the perturbation response of a single-wavelength ϕ-OTDR signal analyzed as a unidimensional speckle pattern, monotonic change in temperature has been measured [10]. A method which exploits the frequency shift concept in [9] has also been used to implement a sensing scheme which involves chirping of the probing pulse, thereby sending the equivalent of pulses with multiple frequency content in one round-trip-time [11,12]. The longitudinal shift of the traces in the spatial domain is related to the magnitude of a local disturbance, and is then used to quantify the local perturbation. Using this technique, it is possible to quantify the change in sign of the perturbation. Owing to the necessity to introduce a given chirp slope within the pulse width, a high bandwidth-to-spatial-resolution ratio is required, where a 13 GHz photodiode and a sampling rate of 40 GHz were used with 10 m spatial resolution. Note that, even though the chirp slope and pulse width determine the range of pulse frequency shift which can be accommodated, the dynamic range of the phase change measurement can be much higher than the spectral content of the pulse. A more recent scheme employs an alternating dual frequency pulse probe for the tracking of the relative shift of two groups of backscattering traces at a given location by computing a correlation between them [13]. This technique avoids the coupling between spatial resolution and dynamic range present in [11], while the use of alternating frequency pulses reduces the measurement speed by half and demonstrated measurements are slow changes in temperature gradient. Another phase demodulation technique involves the use of a local oscillator and 90° hybrid to extract the two orthogonal components of the phase. A technique which uses a 3x3 coupler for demodulating the phase has also been proposed and demonstrated [14,15]. This scheme requires the use of three photodiodes working in full synchronization and an interferometric system which should be kept in thermal isolation for stable demodulation. Another configuration which emulates demodulation in an optical coupler with three pairs of pulses, each of which has a relative phase shift of $2\pi/3$ with respect to each other has also been proposed. This technique addresses the thermal isolation, synchronization and receiver duplicity issues in using a 3x3 coupler but results in a three-fold reduction in the sensing bandwidth [16]. In schemes using a 3x3 coupler and 90° degree hybrid, backscattering intensity fluctuations introduce errors in the demodulated phase and handling them requires additional techniques. Note that demodulation techniques based on coherent detection or using 90° degree hybrid employ the arctan or the four quadrant arctan functions, both of which require unwrapping algorithms for values of the phase outside their corresponding ranges. Unwrapping of a fast, abrupt changing phase is computationally costly, and in the case of distributed sensing such as ϕ-OTDR, it involves more costly two-dimensional unwrapping computations.

In this contribution, we propose the use of a novel ϕ-OTDR sensor based on a double pulse probe and direct detection for distributed dynamic phase change extraction using a stable interferometric demodulation technique which is highly suitable for distributed sensing. Our technique hinges on the observation that distributed information on the phase change along a sensing fiber can be extracted in a simple ϕ-OTDR configuration if a simplified distributed interferometer scheme equivalent to a standard point interferometer such as the 3x3 coupler can be implemented together with a demodulation technique suitable to a distributed scenario. Specifically, in our scheme, a phase generated carrier for every point in the sensing fiber is obtained by sending a pair of coherent pulses into the sensing fiber in such a way that the phase in one of them is modulated with an arbitrary depth. Subsequently, the resulting beating between the backscattering signals from the two probe pulses can act as a radiofrequency carrier of arbitrary phase changes due to distributed external impact on the fiber. After a simple direct detection using a pin photodiode, homodyne demodulation of the phase is done using a technique which is highly suitable for distributed sensing by being

stable for arbitrary values of the modulation depth, independent of the received signal intensity fluctuation and mixing efficiency, and convenient for analogue signal processing. In the following sections, we first discuss the mechanism of using the dual pulse ϕ-OTDR as a distributed interferometer, and present the mathematical background of the enhanced homodyne demodulation scheme used. We then present the experimental setup used to validate our proposed sensing scheme, and describe the experimental results confirming the ability of the sensor to quantify the magnitude of a generic dynamic phase change induced by a non-linear PZT actuator, including comparison of the response with an FBG sensor using a commercial FBG reading unit.

2. Double-pulse ϕ-OTDR and phase generated carrier demodulation

Dynamic phase extraction from just a single disturbance point along an optical fiber can be done using interferometric techniques for quantifying phase changes [17–20], while concurrent demodulation of phase changes from multiple impact points with interferometric configurations requires the use of additional complex setups [21,22]. A similar demodulation can be performed in ϕ-OTDR using a double pulse probe, in which first a pair of adjacent pulses is sent into the sensing fiber and the interaction between the backscattering from the two pulses is used to extract distributed phase changes [16]. The basic schematic of the specific double pulse technique used in the proposed sensor is depicted in Fig. 1, which shows the backscattering signal from two adjacent points traversed by the double pulse indicated along the fiber with positions m and k separated by a short distance Δz, where one pulse is selectively modulated with a phase of $\Delta\delta(t)$. When an external perturbation introducing phase change $\phi(t)$ is applied on a region between these two points, the backscattering from each position $E_{m,k}(t)$ at the receiver has an electric field given by:

$$\begin{aligned} E_m(t) &= E_m \exp[j\delta_m(t) + j\varphi_m], \\ E_k(t) &= E_k \exp[j\phi(t) + j\delta_k(t) + j\varphi_k], \end{aligned} \tag{1}$$

where $E_{m,k}$ are the amplitudes of the fields and $\delta_{m,k}(t)+\varphi_{m,k}$ are the phases in the two locations, $\varphi_{m,k}$ being the initial phases. Note that the term $\phi(t) = f(\xi(t))$ is the phase change which is a function of the external perturbation $\xi(t)$ and appears in the expression for the field term for position k but not that of m. Due to the coherence of the source, the two fields in (1) interfere with each other and the resulting intensity at the receiver will have the expression:

$$I = E_m^2 + E_k^2 + 2E_m E_k \cos(\Delta\delta(t) + \phi(t)), \tag{2}$$

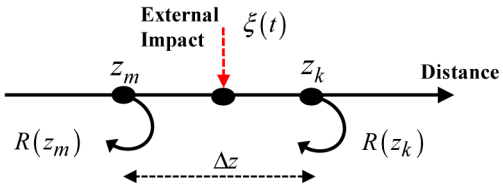

Fig. 1. Schematic of a double pulse ϕ-OTDR showing the backscattering from two adjacent points.

where $\phi(t)$ is the measured phase change between the two positions in the presence of the external impact, $\Delta\delta(t) = C\cos\omega_0 t$, C being the modulation depth and ω_o the modulation angular frequency, is the relative phase change between the two positions. Hence, (2) shows that the double pulse configuration effectively changes the ϕ-OTDR configuration to that of an interferometer for each spatial point, where the resulting beating signal contains the phase

Optics EXPRESS

change due to the external impact information, which can further be extracted using a proper demodulation technique. In our proposed scheme, we use a phase-generated carrier (PGC) demodulation scheme which is highly suitable to distributed sensing to extract the phase. The principle of phase extraction using a generic PGC demodulation technique can be explained by considering the general case of a phase modulated signal with arbitrary phase $\theta(t) = C\cos\omega_0 t + \phi(t)$, which as given in (2) is the phase change in the interfering signal [23]. The detected intensity in the presence of an external impact inducing a phase change of $\phi(t)$ can be written as:

$$I = A + \eta B\cos\left(C\cos\omega_o t + \phi(t)\right). \tag{3}$$

The terms A and B are parameters which depend on the input optical power at the receiver, A being the DC component while B is the amplitude and η stands for the mixing efficiency of the interferometer. Expanding the second term in (3) using the cosine of sums property yields:

$$I = A + \eta B\left\{\cos\left(C\cos\omega_0 t\right)\cos\phi(t) - \sin\left(C\cos\omega_0 t\right)\sin\phi(t)\right\}. \tag{4}$$

The term with a linear multiplication inside cosine and sine functions can be expanded since for any constant C, the Bessel's expansions of nested sine and cosine functions are [23]:

$$\cos\left(C\cos(x)\right) = J_0(C) + 2\sum_{n=1}^{\infty}(-1)^n J_{2n}(C)\cos(2nx), \tag{5}$$

$$\sin\left(C\cos(x)\right) = 2\sum_{n=0}^{\infty}(-1)^n J_{2n+1}(C)\cos((2n+1)x), \tag{6}$$

where $J_n(C)$ is n-th order Bessel function of C. Substituting the terms in (5) and (6) in their respective positions in (4) and using $x = \omega_0 t$ yields a sum of two terms for the intensity:

$$I = A + \eta B[\Phi_1 + \Phi_2]. \tag{7}$$

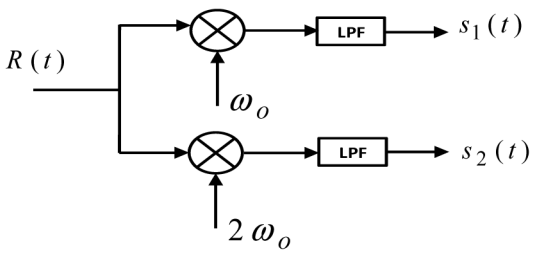

Fig. 2. Initial mixing in PGC demodulation to obtain intermediate signals to the I and Q components (LPF: Low-pass Filter).

The terms Φ_1 and Φ_2 in (7) are two orthogonal components given by [23]:

$$\Phi_1(t) = [J_0(C) + 2\sum_{n=1}^{\infty}(-1)^n J_{2n}(C)\cos(2n\omega_o t)]\cos\phi(t). \tag{8}$$

$$\Phi_2(t) = [2\sum_{n=0}^{\infty}(-1)^n J_{2n+1}(C)\cos((2n+1)\omega_o t)]\sin\phi(t). \tag{9}$$

From (8), it can be seen that when $\phi(t)$ is zero, the component $\Phi_1(t)$ is non-zero, while $\Phi_2(t)$ in (9) vanishes. In contrast, when $\phi(t) = \pi/2$, $\Phi_2(t)$ is non-zero while $\Phi_1(t)$ is

Optics EXPRESS

eliminated. These are signals centered at the even and odd multiples of ω_0. It is also worth noting that $\phi(t)$ itself can be expanded for the generic case of a phase change with amplitude D and angular frequency ω such that $\phi(t) = D\cos(\omega t) + \zeta(t)$. In a fiber interferometric system, the interference signal at the receiver $R(t)$ is used to retrieve the two intermediate components, which are obtained by mixing the incoming signal with two oscillators at ω_0 and $2\omega_0$ followed by low pass filtering as shown in Fig. 2. These signals are then processed according to a PGC demodulation algorithm to obtain the desired phase change. Considering a generic case with interference visibility η and respective carrier amplitudes G and H, the two signals at the receiver in Fig. 2 can be written as:

$$\begin{aligned} s_1(t) &= -\eta BGJ_1(C)\sin\phi(t). \\ s_2(t) &= -\eta BHJ_2(C)\cos\phi(t). \end{aligned} \tag{10}$$

A commonly used scheme is the PGC-arctan method which uses the inverse tangent of the ratio of the two components. The PGC-arctan algorithm is used to retrieve the phase $\phi(t)$ by just performing the inverse tangent of the ratio of the two terms in (10), with the requirement that the value of C, the modulation depth, must be such that $J_1(C) = J_2(C)$ which is true for a value of C = 2.63. With this condition, and for equal amplitudes G and H, the demodulated phase is reduced to the direct inverse tangent of the ratio of $s_1(t)$ and $s_2(t)$. Light Intensity Disturbance (LID) is negligible due the elimination of the amplitudes of the two components with the ratio. However, the deviation of the modulation depth value from 2.63 introduces errors in demodulation and studies have shown that it is not the optimum condition for reducing the demodulation error [24,25], as slight deviations from this value have been shown to result in reduced accuracy in the phase measurement [26,27].

In addition, this technique involves phase unwrapping for values of the phase outside the range of the arctan function to eliminate discontinuities with a suitable algorithm. Multi-dimensional phase unwrapping, especially when fast jumps of the instantaneous phase exist, is a computationally intensive algorithm, and has been a subject of a number of independent investigations in the past [28,29] including recent ones [30–32]. This technique has been used in discrete sensing schemes including those based on interferometry. Even though fringe counting algorithms can be used for slower and less abrupt changes, note that the use of unwrapping in distributed sensing introduces computations of two-dimensional phase unwrapping such as the ones required in image processing schemes [33–35]. Since the amount of data that can be handled by a DAS in any monitoring scenario remains one of the main challenges in future DAS solutions according to recent DAS market forecast [2], the adoption of any interferometry demodulation scheme, including application of PGC to a DAS system, requires a close consideration of the associated digital signal processing and storage. Another commonly used PGC demodulation technique is the differentiate-and-cross-multiply (PGC-DCM) scheme where the phase is obtained by differentiating each of the components $s_1(t)$ and $s_2(t)$ and cross multiplying them before taking their difference. Applying this scheme to the intermediate components in (10), and using trigonometric identity, we first obtain [27]:

$$\begin{aligned} s_{DCM}(t) &= [B^2\eta^2 GHJ_2(C)J_1(C)]\times \\ &\quad [\sin^2\phi(t) + \cos^2\phi(t)]\dot{\phi}(t) \\ &= B^2\eta^2 GHJ_2(C)J_1(C)\dot{\phi}(t). \end{aligned} \tag{11}$$

Optics EXPRESS

Integration of the last term in (11) gives the final phase multiplied with the remaining terms:

$$s_{DCM}(t) = B^2\eta^2 GHJ_2(C)J_1(C)\phi(t). \tag{12}$$

It can be seen from (12) that the main issue with the PGC-DCM technique is that, while the Bessel function terms of the modulation depth are mere linear multiplication factors, there is clear dependence of the demodulated phase on the square of the B value and mixing efficiency η. This contributes to detrimental light intensity disturbance (LID), incurring significant errors in demodulation, and requires techniques including normalizing, (which introduces distortions) or tracking the intensity and using feedback loops to reduce [26].

3. Stable PGC demodulation with a double-pulse ϕ-OTDR scheme

In the proposed sensing scheme, we use an enhanced phase demodulation technique which addresses the aforementioned issues in conventional PGC phase extraction methods to extract the dynamic phase change in the backscattering from the double pulse probe. The technique involves an enhanced PGC demodulation with Differentiate Multiply and Square (PGC-DMS) method whose basic mechanism is depicted in Fig. 3 [27]. As shown, the instantaneous phase is obtained from the intermediate components by first differentiating $s_1(t)$ and multiplying it by $s_2(t)$ and then dividing the result by the square of $s_2(t)$. When applied to the two intermediate terms at the receiver given in (10), first the product and square terms become:

$$\begin{aligned} s_{D1}(t)s_2(t) &= (\eta B)^2 GHJ_1(C)J_2(C)\cos^2\phi(t)\frac{d}{dt}\phi(t), \\ s_{SQ2}(t) &= (\eta BH)^2 J_2^2(C)\cos^2\phi(t). \end{aligned} \tag{13}$$

Subsequently, taking the ratio of the terms in (13) and assuming equal amplitudes G and H in the mixing carriers gives:

$$\frac{s_{D1}(t)s_2(t)}{s_{SQ2}(t)} = \frac{J_1(C)}{J_2(C)}\frac{d}{dt}\phi(t). \tag{14}$$

Since the instantaneous phase contains both the high frequency perturbation and low frequency environmental drift, it will have the form $\phi(t) = D\cos(\omega t) + \zeta(t)$. Any phase change can hence be obtained by first integrating (14) and then as appropriate, high-pass filtering the result to remove slow environmental drifts:

$$S_{DMS}(t) = \int \frac{J_1(C)}{J_2(C)}\frac{d}{dt}\phi(t)\ dt = \frac{J_1(C)}{J_2(C)}\phi(t) \tag{15}$$

As can be clearly seen from (15), the ratio of the two Bessel functions for any value of the modulation depth C remains a mere linear multiplication factor, while both terms B and η, which are difficult to control if the PGC-DCM algorithm is used, are eliminated. This method greatly suppresses the LID, which would significantly affect the results of the phase demodulation. It is also demonstrated to exhibit enhanced suppression of the total harmonic distortion compared to the PGC-arctan and PGC-DCM methods [27]. Note that light intensity disturbance due to backscattering signal fluctuations is an issue in a number of existing ϕ-OTDR demodulation methods and requires additional techniques in order to be suppressed [14,16].

Optics EXPRESS

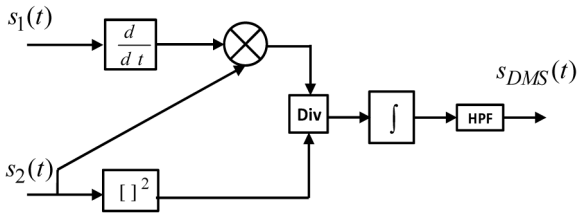

Fig. 3. Phase demodulation in the ϕ-OTDR sensor using PGC-DMS.

Hence, PGC-DMS demodulation mitigates the requirement to limit the modulation depth to a fixed value, doesn't require phase unwrapping and is robust to LID, making it highly suitable for use in demodulation in ϕ-OTDR. Note also that the integration and differentiation functions involved in the PGC-DMS demodulation used in our technique can be easily implemented using operational amplifiers, which are fundamental building blocks of analogue signal processing systems [36]. This offers an advantage in terms of required digital storage and processing in distributed fiber optic sensing systems in which very often large volumes of data from multiple points are involved. This demodulation scheme is also a promising candidate for use with integrated analogue systems, since operational amplifies are available in CMOS integrated circuits [37,38], whose enabling technology is also compatible with silicon photonics [39], allowing hybrid platforms which combine electrical and photonic circuits for a compact integrated receiver [40]. Hence, the demodulation scheme used in the proposed ϕ-OTDR sensor is highly suitable for distributed dynamic phase extraction.

4. Experimental setup

The experimental setup used to demonstrate the proposed sensing scheme is shown in Fig. 4. First, the light from a narrowband laser with a linewidth of ~50 kHz is amplified using an Erbium-Doped Fiber Amplifier (EDFA) to boost the power level and an Optical Band-pass Filter (OBPF) is used to filter out the ASE noise. The signal is then sent into an Acousto-optic Modulator (AOM) which generates an initial single pulse.

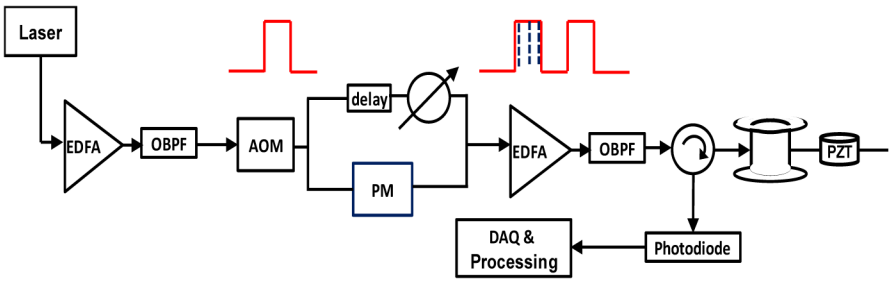

Fig. 4. Experimental setup of the proposed ϕ-OTDR sensor.

The straightforward way to selectively modulate the phase of one of two consecutive optical pulses would have been to generate a double pulse in the AOM and use delay synchronization to selectively apply phase modulation to only one of them. However, in our scheme, we propose a more robust method starting from a single pulse and generating a pair of leading and trailing pulses. This is done by first generating one single pulse using the AOM, and then using a splitter and adding a fiber delay and a Variable Optical Attenuator (VOA) in one arm and a Phase Modulator (PM) in the other. The PM is modulated with sinusoidal voltages with a typical frequency of 10 kHz and an arbitrary modulation depth. The VOA is used to adjust the powers of the two pulses to equal levels, while it can also be used to suppress the pulse passing through the same arm, whenever the need to use only a single pulse arises. This configuration guarantees that, for any repetition rate of the signal

Optics EXPRESS

used to drive the PM, the pulse that is selectively phase modulated is precisely the trailing one. The PM and AOM are driven with WFGs which are synchronized to the triggering of the acquisition system. The selectively phase modulated pulse pair is then further amplified and boosted using a second EDFA and OBPF pair before the double pulse probe is sent into a 1.5 km long singlemode sensing fiber via a three port optical circulator. At the end of the fiber, a nonlinear PZT actuator is used to induce a controlled external vibration. The PZT is driven by a voltage amplifier to which RF signals of controlled frequency and amplitude can be applied. The backscattering from the fiber passes through the return port of the circulator and is then coupled into a simple direct detection receiver which uses a 125 MHz PIN photodiode. The signal is then acquired in real time with a fast acquisition system with embedded ADC. While the measurement of an individual trace can be done in just a round-trip-time of the fiber, typical measurements of vibrations involve hundreds of individual acquisitions at rates of 50 kHz (RTT = 20 μs). Then, the acquired traces were rearranged to form a matrix of traces with each row representing an entire trace of the whole fiber and each column the evolution of the phase modulated signal for each spatial location. Subsequently, mixing with the RF signal which is used to modulate the PM and filtering were employed to obtain the intermediate signals $s_1(t)$ and $s_2(t)$ described in Fig. 2, followed by the application of the PGC-DMS demodulation scheme shown in Fig. 3 to extract the dynamic phase change.

Note that the number of traces acquired for measuring the transient signal is programmable and it depends on the vibration frequency and the number of cycles that need to be measured. The maximum number of acquired traces along the whole sensing distance is determined by the sampling rate and the memory of the real time acquisition system. Continuous acquisition to observe many cycles of a low frequency transient signal is possible by limiting the trace acquisition to a short section of the fiber near the PZT. Besides, the maximum measurable frequency of the phase change when using PGC depends on the frequency of the signal used to modulate the phase of one of the pulses. Typically, for sensing distances of less than 1 km, phase modulation frequencies of 10s of kHz can be used.

5. Experimental results and discussions

To test the effect of phase modulation on the backscattering traces in the proposed scheme for phase demodulation, first pulses are sent into a 1 km test fiber when the PM is driven with a high-frequency RF signal with arbitrary modulation depth. The acquired individual traces are depicted in Fig. 5, clearly showing the effect of phase modulation in one of the pulses on the backscattering trace. The plot shows traces for single pulse with and without phase modulation and those of a double pulse with and without selective modulation of the phase in one of them. It can be seen that the double pulse scheme results in the mixing of the backscattering from the two pulses. In addition, the phase modulation of the pulse alters the pattern of the coherent speckles in both single and double pulse traces. In both the single and double pulse responses, the spatial resolution remains the same with application of phase modulation. After observing the effect of selective phase modulation on one pulse for individual single traces, the exact time evolution of the modulation needs to be measured for different phase modulation frequencies of the PM. This is done by continuously acquiring a number of traces with the double pulse and selective phase modulation and observing the backscattering signal for multiple locations when no perturbation is applied.

Optics EXPRESS

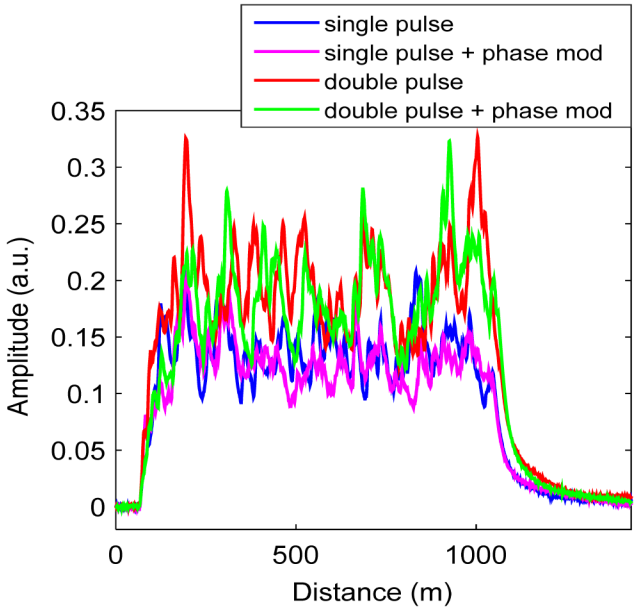

Fig. 5. Individual ϕ-OTDR traces for single and double pulse both with and without selective phase demodulation of one pulse.

The observed spectra for any arbitrary position along the fiber are shown in Fig. 6 when 5, 8 and 10 kHz modulating signals are used at the PM. As can be clearly seen, the phase modulation appears for each spectrum at the corresponding modulation frequency. Note that this modulation is observed in the coherent Rayleigh backscattering traces acquired after sending the double pulse, and it exists at all locations along the whole fiber, confirming the coherent mixing of the backscattering signals from the two pulses and the availability of the desired carrier wave for distributed dynamic phase change. Note that there are no applied vibrations and the measured phase change here is due to slow environmental drifts which are static within the short span of the measurement.

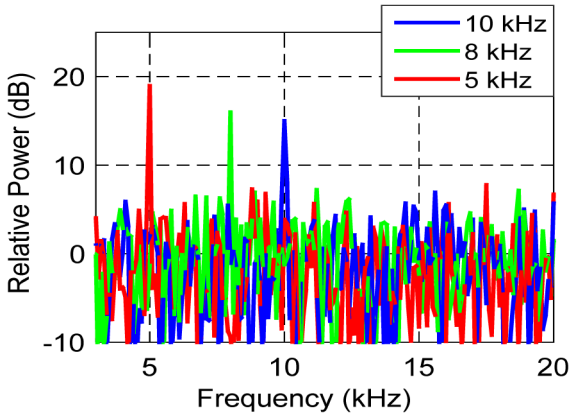

Fig. 6. Spectra of acquired signal with no perturbation at an arbitrary locations showing corresponding carriers resulting from selective phase modulation of one of the pulse pairs with 5, 8 and 10 kHz signals.

Then, 1 and 2 kHz vibration signals were applied to the nonlinear PZT actuator placed at 1.5 km, and the phase modulated signals were observed before applying the mixing, filtering and PGC-DMS demodulation. Sample spectra of such a signal are shown in Fig. 7 and their

Optics EXPRESS

observations show that the induced dynamic impact appears in sidebands to the 10 kHz, which is the RF signal used to modulate the phase of one of the pulses, and 20 kHz carriers at steps of 1 and 2 kHz. This is consistent with the spectrum of a generic phase-modulated signal, which contains tones spaced at intervals of the modulating frequency and centered at the carrier frequency. Since there is an induced dynamic phase change, as opposed to the case in which there are no applied vibrations, it is now possible to see the orthogonal components centered at ω_0 and $2\omega_0$, which are 10 and 20 kHz, respectively.

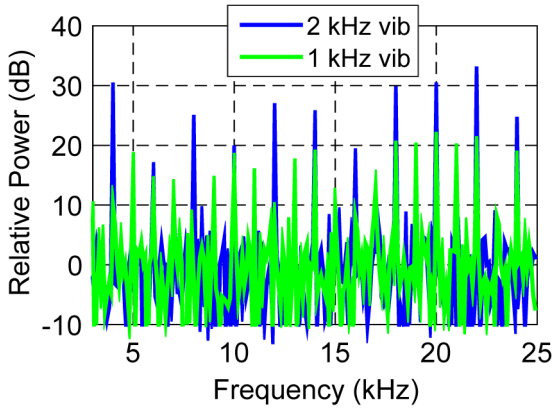

Fig. 7. Modulated signals showing raw perturbation signals when 1 and 2 kHz vibrations applied to the PZT, before performing the mixing, filtering and PGC-DMS demodulation operations.

Subsequently, the modulated signal is first mixed with the RF signals used in the phase demodulation and then low-pass filtered to obtain the intermediate signals. These spectra are obtained directly from the evolution of the intensity of the backscattering signal and are shown here before mixing, filtering and demodulation operations. Note that acoustic signals from naturally occurring vibrations that could be of interest in a real world monitoring scenario are known to have multiple frequency components. When any external impact is applied on a structure from a vibration source, standard parameters such as the peak sound pressure (PSP), are used to quantify the intensity of the signal [41,42]. The PSP is a function of the RMS value of the sound, which in turn scales with the energy in the fundamental and the harmonic frequencies.

The best way to confirm the ability of our proposed scheme to perform quantitative measurement of phase changes due to vibrations is therefore to prove its capacity to extract the dynamic response of the demodulated phase from an external impact due to a multi-spectral perturbation and compare it with an external sensor. We used the nonlinear PZT actuator having responses with higher harmonics, and demodulated the dynamic phase change using the PGC-DMS scheme shown in Fig. 3. The extracted phase change in time domain when the PZT is driven with a sample 2 kHz input is shown in Fig. 8(a). The result shows the effectiveness of the technique to extract the dynamic phase change induced by the nonlinear PZT, as is evident from the power spectrum of the signal shown in Fig. 8(b). Even though the reported dynamic phase change has amplitude less than π, the proposed method is used to detect phase changes above this range introduced by environmental drifts, which have been high-pass filtered, without requiring unwrapping. Note that the nonlinearity of the vibrations from PZT actuators are well known and the associated harmonics in dynamic operations have been the subject of independent studies [43], including use of Bessel function based analysis and experimental evaluation of the higher order harmonics [44]. Precise characterization of the harmonics of these vibrations is also critical to the accurate use of PZT in dynamic control systems. We have done measurements of dynamic phase changes induced by the PZT with

Optics EXPRESS

stronger higher order harmonics, and a sample spectrum of the demodulated phase when the PZT is driven with a larger peak-to-peak voltage is also depicted in Fig. 9, where the SNR of the demodulated phase is ~24.16 dB. This further shows that the proposed dual pulse scheme with selective phase modulation and PGC-DMS demodulation can extract fundamental and higher order frequency components of natural perturbations required in the construction of the original dynamic response.

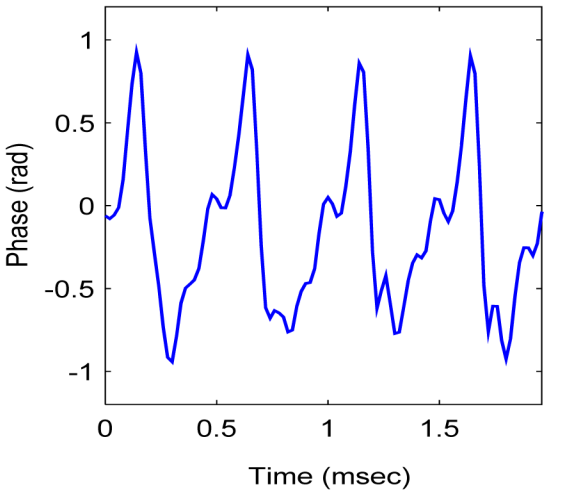

(a)

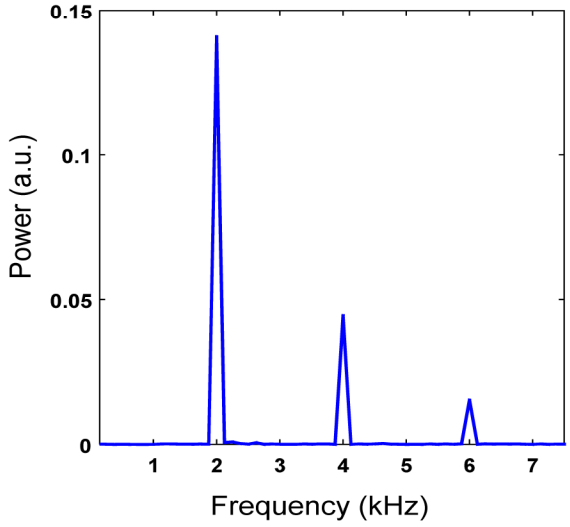

(b)

Fig. 8. (a) Demodulated phase change for 2 kHz vibration applied to the PZT and (b) The spectrum of the demodulated phase change with PGC-DMS showing higher order harmonics of the response.

The nonlinear characteristics of the PZT are also confirmed by measuring the response with a point sensor based on an FBG and a commercial reading unit. To do the characterization of nonlinearity, first an FBG is closely attached to the PZT actuator, and one of its ends is connected to the through end of a three-port circulator. Using a broadband source as the driving signal at the circulator's input, the spectral shift of the reflected light from the FBG is measured using a BaySpec Inc. reading unit. Since the reading unit has a

maximum sampling rate of 5 kHz (for an effective measurement up to vibration frequency of 2.5 kHz), the characterization of the actuator's harmonics is performed using a 600 Hz input to the PZT. The conversion of the measured wavelength shift to strain for the FBG is made using a wavelength shift per strain of 1.2 pm/$\mu\varepsilon$, while for the ϕ-OTDR sensor, the relation between the demodulated phase change and the strain $\Delta\phi(t) = \varepsilon\Delta L(2\pi n/\lambda)\times 0.78$ is used where ε is the strain, ΔL is the relative interference path delay, λ being the wavelength, and n the refractive index [15]. Note that the factor 1.2/1.55~0.78 is used in the calculation of the strain and the remaining 22% of the phase change is due to change in refractive index caused by strain [15]. The measured responses of the PZT using both the BaySpec and DAS measurements are shown in Fig. 10. It can be seen that the higher order harmonics of the PZT response at 1200 and 1800 Hz are clearly observed in both measurements, further confirming the distribution of the power among the different frequency components, and hence the capability of the proposed scheme to quantify the dynamic phase change induced by an arbitrary perturbation source.

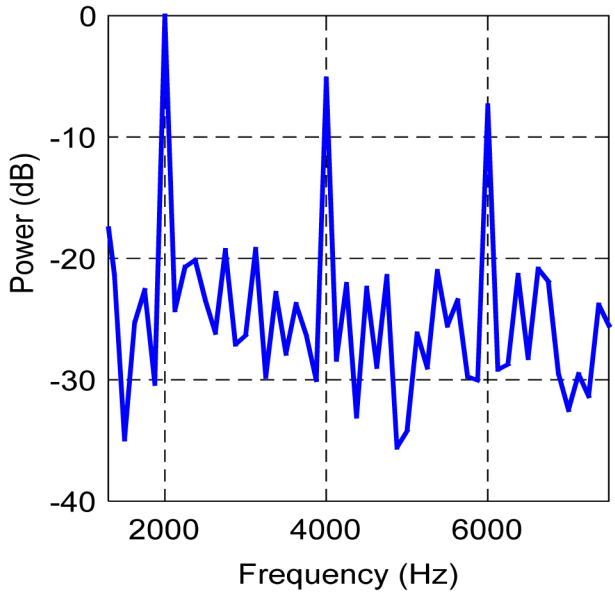

Fig. 9. Spectra of demodulated phase using dual pulse probe with PGC-DMS demodulation.

Note that comparison of the spectra of the responses is shown since the capability of the proposed scheme to detect the multi-frequency response of the PZT is more clearly visible in the frequency domain. In addition, the linearity of the system is confirmed by the similarity of the responses obtained using the FBG sensor and PGC-DMS demodulation. This is also evident in the consistency of the minima and maxima of the sinusoidal response of the demodulated phase given in Fig. 8(a). Note also that spectra of dynamic phase changes have been observed at peak-to-peak PZT driving voltage levels which are two orders of magnitude below the one reported in Fig. 8(a), enabling sensitivities in the orders few 10s of milliradians.

The proposed ϕ-OTDR sensor involves homodyne demodulation with a PIN photodiode of only 125 MHz bandwidth, while enabling a high-speed dynamic measurement. The theoretical limit to the measurable speed of phase change is set by the measurement rate of the ϕ-OTDR scheme; for example, with an RTT of 20 μs corresponding to 50 kHz sampling rate, a phase modulation of up to 25 kHz can be used. This enables measurements with a high speed per detection bandwidth and complexity of optical receiver compared to most

conventional ϕ-OTDR demodulation schemes, making the proposed scheme a preferable technique for use in cost-effective dynamic monitoring systems.

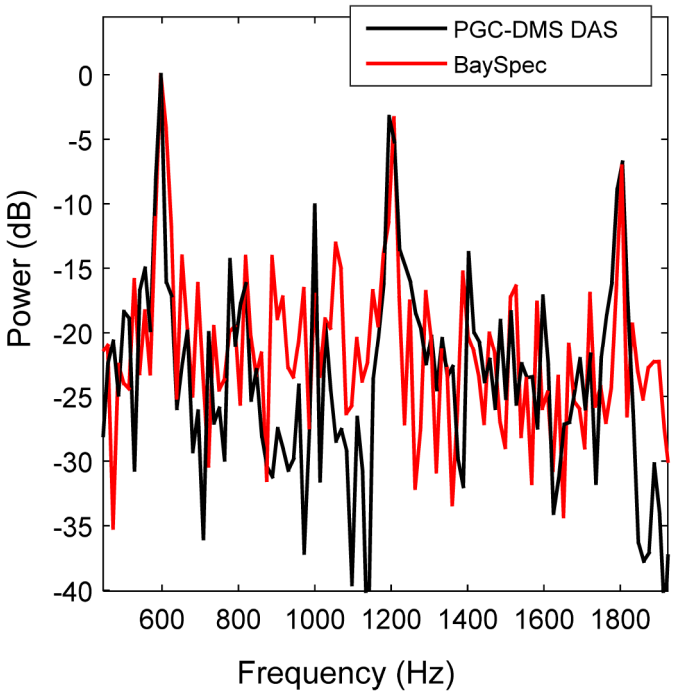

Fig. 10. Comparison of the response of a nonlinear PZT actuator using proposed PGC-DMS scheme for DAS with that of a point sensor and a commercial reading unit.

6. Summary

We have proposed and experimentally demonstrated a ϕ-OTDR scheme for dynamic phase measurements using a double pulse probe and a simple direct detection receiver based on a pin photodiode with a bandwidth of 125 MHz. The selective modulation of the phase of one of the probing pulses is proven to generate a carrier in the backscattering signal for arbitrary perturbations along the fiber. A stable homodyne demodulation scheme with an arbitrary phase modulation depth is used to extract distributed dynamic phase changes along the fiber. The demodulation method employed in the sensor is highly compatible with distributed dynamic monitoring systems by being robust against backscattering light intensity changes, not requiring computationally costly two-dimensional phase unwrapping and involving computations which can also be implemented using analogue signal processing.

The proposed technique is used to measure a 2 kHz dynamic phase change induced by a nonlinear PZT actuator placed at a distance of 1.5 km with an SNR of 24.16 dB, demonstrating its capability to make quantitate measurements of dynamic phase changes from a generic external impact. The characterization of the nonlinear response is further confirmed by comparing the demodulated response of the PZT with one obtained using an FBG-based sensor. Finally, the proposed ϕ-OTDR demodulation scheme offers a high speed per detection bandwidth and receiver complexity making it suitable for use in cost-effective distributed dynamic monitoring systems.